

# Efficient computation of delay differential equations with highly oscillatory terms

Marissa Condon  
School of Electronic Engineering  
Dublin City University  
Dublin 9, Ireland

Alfredo Deaño  
Dpto. de Matemáticas  
Universidad Carlos III de Madrid,  
Avda. Universidad, 30, Leganés 28911, Madrid, Spain

Arieh Iserles  
Department of Applied Mathematics and Theoretical Physics  
Centre for Mathematical Sciences  
University of Cambridge  
Wilberforce Rd, Cambridge CB3 0WA, UK

Karolina Kropielnicka  
Department of Applied Mathematics and Theoretical Physics  
Centre for Mathematical Sciences  
University of Cambridge  
Wilberforce Rd, Cambridge CB3 0WA, UK

and  
Institute of Mathematics,  
University of Gdańsk,  
Wit Stwos Str. 57, 80-952 Gdańsk, Poland

March 18, 2011

## Abstract

This paper is concerned with the asymptotic expansion and numerical solution of systems of linear delay differential equations with highly oscillatory forcing terms. The computation of such problems using standard numerical methods is exceedingly slow and inefficient, indeed standard software is practically useless for this purpose. We propose an alternative, consisting of an asymptotic expansion of the solution, where each term can be derived either by recursion or by solving a non-oscillatory problem. This leads to methods which, counter-

intuitively to those developed according to standard numerical reasoning, exhibit improved performance with growing frequency of oscillation.

## 1 Introduction

There is a growing interest in the numerical solution of differential equations with high oscillatory solutions, motivated in large measure by their very wide range of applications in mathematical modelling (Engquist, Fokas, Hairer & Iserles 2009). Such equations come in two basic ‘flavours’: the oscillation can originate either in intrinsic features of the underlying differential problem (Cohen, Hairer & Lubich 2005) or in the presence of a highly oscillatory forcing term (Calvo & Sanz-Serna 2010, Condon, Deaño & Iserles 2010*b*).

A rich source of highly oscillatory problems with extrinsic oscillation (i.e., when the oscillation originates in a forcing term) is computational electronic engineering. The eternal quest for accurate models has led to an increasing interest in delay differential equations for engineering applications. Delays arise in whenever signals are transmitted over a finite distance from one point to another, so accurate models of communication systems inevitably should include delay differential equations. In their paper Kyrychko & Hogan (2010) provide a vast array of applications of delay differential equations in engineering. Some applications worth highlighting include laser dynamics (van Wiggeren & Roy 1998) and the related secure communication techniques using chaos (Udaltsov, Goedgebuer, Larger, Cuenot, Levy & Rhodes 2003). Analysis of coupled microwave oscillators also requires the inclusion of delays as frequencies are above 10GHz in such systems (Wirkus & Rand 2002), consequently the time for light to travel the typically few centimetres between the oscillators is significant. Chembo, Larger & Colet (2008) specifically mention the difficulties in relation to numerical analysis of optoelectronic microwave oscillators. These state of the art microwave generators are increasingly of interest in the area of high-precision radar and sensor technology and accurate efficient numerical simulation is crucial for efficient engineering design.

The modelling of highly oscillatory electronic circuits results in ordinary, partial, differential-algebraic and delay differential problems. While our understanding of ordinary differential equations with extrinsic oscillation has advanced greatly following recent research and effective numerical methods are available (Chartier, Murua & Sanz-Serna 2010, Condon, Deaño & Iserles 2010*a*), the solution of delay differential equations with highly oscillatory forcing terms is largely unexplored. This paper is devoted to an initial foray into this subject matter and concerns itself with the asymptotic and numerical solution of linear systems of this kind.

More specifically, we are concerned with a system of linear delay differential equations (DDEs) of the form

$$\mathbf{y}'(t) = A\mathbf{y}(t) + B\mathbf{y}(t-1) + \sum_{m=-\infty}^{\infty} \mathbf{a}_m(t)e^{im\omega t}, \quad 0 \leq t \leq T, \quad (1.1)$$

with the initial condition

$$\mathbf{y}(t) = \boldsymbol{\varphi}(t), \quad -1 \leq t < 0, \quad (1.2)$$

where  $\mathbf{y}(t)$ ,  $\mathbf{a}_m(t) : \mathbb{C} \rightarrow \mathbb{C}^d$ ,  $m \in \mathbb{Z}$ , while  $A$  and  $B$  are  $d \times d$  constant matrices. In particular, we are interested in the case when  $\omega \gg 1$ . Note that the forcing term, the origin of rapid oscillations is written in a form of a *modulated Fourier expansion* (MFE). Such expansions have been pioneered by Cohen et al. (2005) in backward error analysis of partial differential equations, subsequently used by Sanz-Serna and his collaborators in their work on the heterogeneous multiscale method (Calvo & Sanz-Serna 2010, Chartier et al. 2010), as well as in our research into different types of extrinsic high oscillations (Condon et al. 2010b, Condon et al. 2010a).

Standard forcing terms, e.g.  $\mathbf{a} \sin \omega t$ , are an obvious special case of an MFE, as are ‘plain’ Fourier series. However, the extra generality afforded by MFE comes at no extra price and, even were we to commence with  $\mathbf{a} \sin \omega t$ , say, MFEs would have anyway appeared in our expansions. Therefore, we may just as well commence from this, more general setting.

There exist numerous methods for the numerical solution of delay differential equations, mostly based upon an extension of key tools in the numerical analysis of ordinary differential equations: Runge–Kutta, collocation and multistep methods (Bellen & Zennaro 2003). However, brief reflection demonstrates that the highly oscillatory nature of the forcing term necessitates the use of an exceedingly small step size. Thus, for simplicity let us assume that we are solving the delay differential problem

$$\mathbf{y}'(t) = \mathbf{f}(t, \mathbf{y}(t), \mathbf{y}(t-1))$$

with the Euler method

$$\mathbf{y}_{n+1} = \mathbf{y}_n + h \mathbf{f}(nh, \mathbf{y}_n, (\lfloor n-M \rfloor - (n-M) + 1) \mathbf{y}_{\lfloor n-M \rfloor - 1} + (n-M - \lfloor n-M \rfloor) \mathbf{y}_{\lfloor n-M \rfloor}),$$

where we have used the constant step  $h = 1/M$ ,  $M \in \mathbb{N}$ , and  $\mathbf{y}_n \approx \mathbf{y}(nh)$ . It is well known that the local truncation error scales like  $h^2 \mathbf{y}''(nh)$ , hence the global error scales like  $h \mathbf{y}''(nh)$ . For the highly oscillatory system (1.1) we have  $\mathbf{f}(t, \mathbf{y}(t), \mathbf{y}(t-1)) = A \mathbf{y}(t) + B \mathbf{y}(t-1) + \sum_{m=-\infty}^{\infty} \mathbf{a}_m(t) e^{im\omega t}$  and it is easy to ascertain that

$$\mathbf{y}''(t) = \frac{d}{dt} \mathbf{f}(t, \mathbf{y}(t), \mathbf{y}(t-1)) \approx i\omega \sum_{m=-\infty}^{\infty} \mathbf{a}_m(t) e^{im\omega t}, \quad \omega \gg 1,$$

scales like  $\omega$ . Therefore, to entertain any hope of reasonable precision we are compelled to choose a very small  $h\omega$ . A similar state of affairs prevails for all integration methods based upon B-series, inclusive of multistep and Runge–Kutta methods and Taylor expansions. Moreover, standard error-control and adaptation techniques, as used in modern advanced ODE and DDE software, are of little use because the error-control mechanism is bound to select a very small step size, consistent with  $h\omega \ll 1$ . Using such methods and software for (1.1) and similar highly oscillatory systems is not just exceedingly slow and expensive but also, once the interval of integration  $[0, T]$  is sufficiently long, leads to substantial roundoff error accumulation and global error in excess of user-supplied tolerance. All this makes a compelling case for the development of a completely different breed of methods, dedicated to highly oscillatory systems and based upon completely different premises.

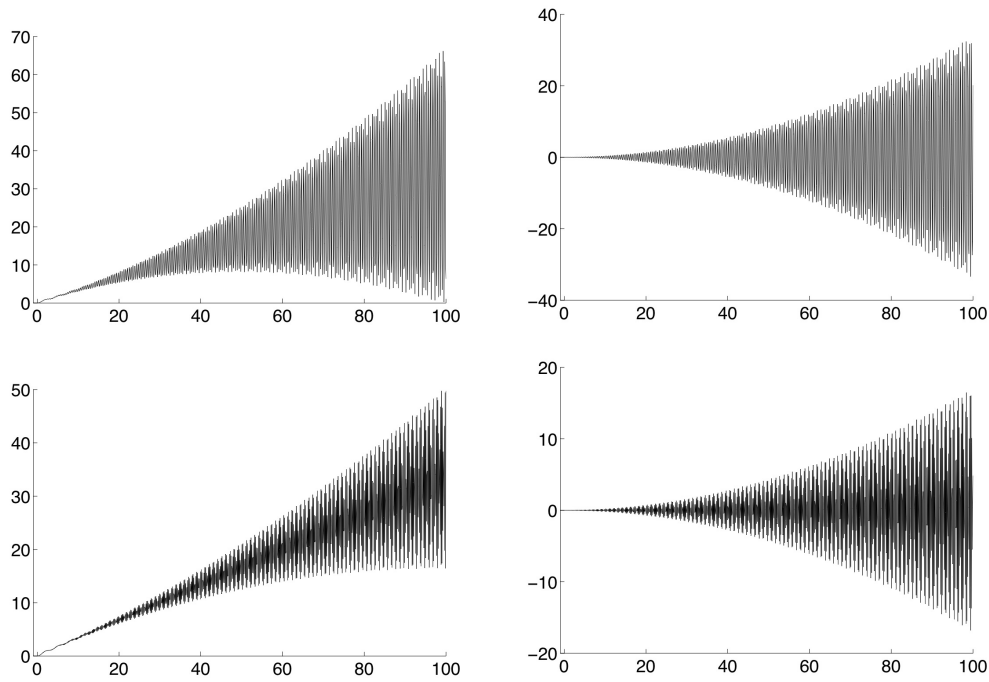


Figure 1.1: Real (on the left) and imaginary (on the right) parts of the solution of (1.3) for  $\omega = 50$  (top row) and  $\omega = 100$ .

To illustrate our point and flesh out some numbers, let us consider the scalar equation

$$\left. \begin{aligned} y'(t) &= -y(t) - 2y(t-1) + t + (t+1)^2 e^{6i\omega t} - i e^{-10i\omega t}, & t \in [0, T], \\ y(t) &= \varphi(t) & t \in [-1, 0]. \end{aligned} \right\} \quad (1.3)$$

The real and imaginary parts of the solution for  $\omega = 50$  are displayed in Fig. 1.1 and, unsurprisingly, they exhibit high oscillation.

We have approximated the solution of (1.3) for  $\omega = 50$  (a fairly gentle oscillation) and  $\varphi \equiv 0$  using standard the MATLAB routine `dde23`, which is an implementation of a Runge–Kutta method with variable step size and error control. The errors for absolute tolerances of  $10^{-3}$ ,  $10^{-6}$  and  $10^{-9}$  are displayed in Fig. 1.2. It is evident that, regardless of user-specified tolerance, `dde23` delivers pointwise error of  $\mathcal{O}(1)$ : not even a single significant digit is recovered correctly. We should perhaps add that the entire pointless exercise took between 628 and 1057 seconds.

For comparison, we have solved (1.3) using the asymptotic-numerical method which we describe in Section 2 for different values of the parameter  $p$ . Not wishing to preempt subsequent discussion, we just observe that  $p$  denotes the number of ‘asymptotic layers’ in the representation of the solution of (1.1). The errors decrease rapidly with

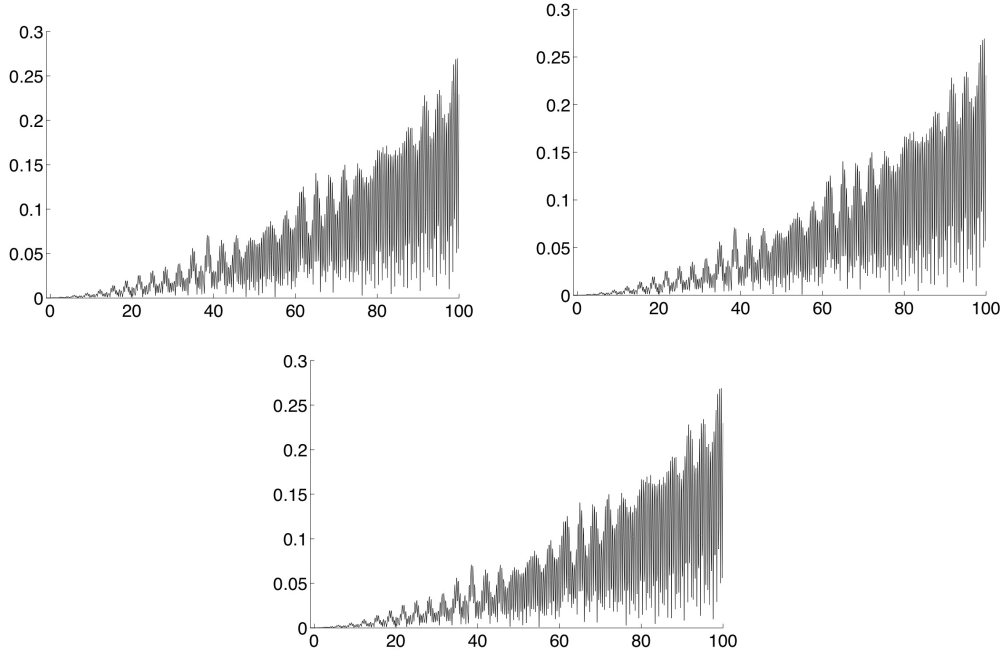


Figure 1.2: Absolute values of errors in the solution of (1.3) with  $\omega = 50$ , using `dde23` with `AbsTol` =  $10^{-3}$ ,  $10^{-6}$ ,  $10^{-9}$ .

$p$  (they grow in time at a similar rate to the growth of  $|y(t)|$ , cf. Fig. 1.1). Note that the run-times of the four methods were just 0.472, 0.810, 1.074 and 1.247 seconds, respectively.

A major feature of the methodology of this paper is that the higher the oscillation, the smaller the error. This is brought home by Fig. 1.4, where we provided the same information as in Fig. 1.3, except that the size of  $\omega$  has been doubled. The run-times are virtually the same as for  $\omega = 50$ : 0.508, 0.779, 0.994 and 1.190 seconds respectively, while the pointwise accuracy improves. It goes without saying that `dde23` delivers an equally useless solution, regardless of user-provided tolerance, in this setting, except that the run-time for  $\omega = 100$  is more than doubled.

Our ultimate goal is to develop asymptotic-numerical methodology for nonlinear equations of the form

$$\mathbf{y}'(t) = \mathbf{f}(t, \mathbf{y}(t), \mathbf{y}(t-1)) + \mathcal{A}_\omega(t)\mathbf{g}(t, \mathbf{y}(t), \mathbf{y}(t-1)), \quad (1.4)$$

where  $\mathcal{A}_\omega$  is a  $d \times d$  matrix with MFE entries,  $(\mathcal{A}_\omega)_{k,\ell} = \sum_{m=-\infty}^{\infty} a_m^{k,\ell}(t)e^{im\omega t}$ , and with the initial condition (1.2). Inasmuch as the solution of linear equations like (1.1) is interesting on its merit, our main concern is in laying the foundations toward asymptotic and numerical solution of nonlinear equations like (1.4).

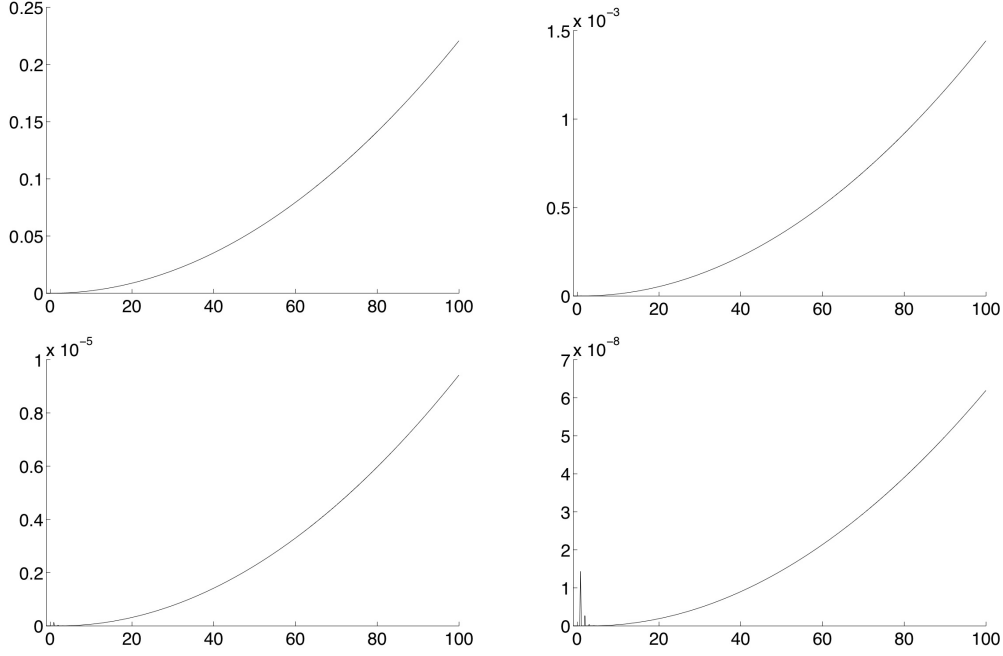


Figure 1.3: Absolute values of errors in the solution of (1.3) with  $\omega = 50$ , using our method with  $p = 1, 2$  (top row) and  $p = 3, 4$ .

## 2 Asymptotic expansion and asymptotic-numerical methods

### 2.1 Asymptotic expansions for ODEs

Our starting point is the highly oscillatory ordinary differential system

$$\mathbf{y}' = \mathbf{f}(t, \mathbf{y}) + \sum_{m=-\infty}^{\infty} \mathbf{a}_m(t) e^{im\omega t}, \quad 0 \leq t \leq T, \quad \mathbf{y}(0) = \mathbf{y}_0, \quad (2.1)$$

whose solution can be expanded asymptotically,

$$\mathbf{y}(t) \sim \mathbf{p}_{0,0}(t) + \sum_{r=1}^{\infty} \frac{1}{\omega^r} \sum_{m=-\infty}^{\infty} \mathbf{p}_{r,m}(t) e^{im\omega t} \quad (2.2)$$

(Condon et al. 2010b). The functions  $\mathbf{p}_{r,m}$  are all independent of  $\omega$ , hence non-oscillatory. For  $m = 0$  they can be obtained by solving a non-oscillatory ordinary differential equation, while for  $m \neq 0$  we find them by recursion. The important feature of (2.2) is thus that its building blocks, the functions  $\mathbf{p}_{r,m}$ , can be derived without any reference to  $\omega$  and the latter enters the calculation only once the asymptotic expansion

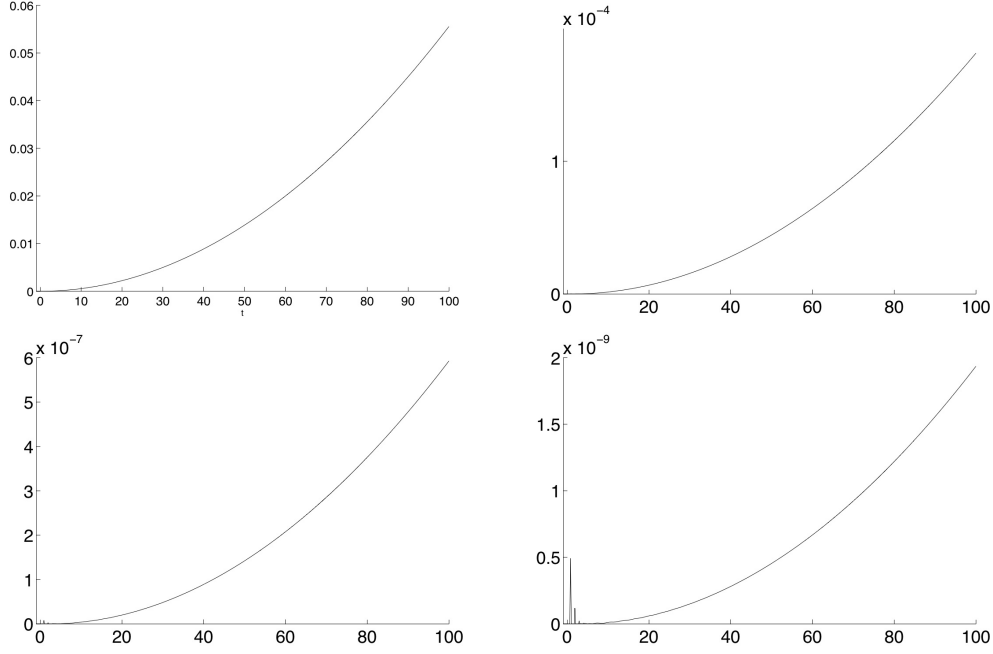


Figure 1.4: Absolute values of errors in the solution of (1.3) with  $\omega = 100$ , using our method with  $p = 1, 2, 3, 4$ .

is computed for a specific value of  $t$ . Therefore, the expansion actually *improves* as  $\omega$  becomes large. This might be surprising to those used to methods based upon Taylor expansions but should come as little surprise to practitioners of asymptotic analysis.

Another important feature of (2.2), which is shared by asymptotic expansions of DDEs, is that the solution consists of amplitude- $\mathcal{O}(\omega^{-1})$  oscillations superimposed upon the non-oscillatory function  $\mathbf{p}_{0,0}$ .

## 2.2 Asymptotic expansion of (1.1)

We wish to emulate the asymptotic expansion (2.2) in the setting of delay differential equations. Unfortunately, this model is much too simple for our needs. Our basic *ansatz*, valid for both the ODE (2.1) and the DDE (1.2) is that

$$\mathbf{y}(t) \sim \mathbf{p}(t) + \sum_{r=1}^{\infty} \frac{1}{\omega^r} \boldsymbol{\psi}_r(t, \omega), \quad \omega \gg 1. \quad (2.3)$$

Note that the  $\boldsymbol{\psi}_r(t)$ s depend on  $\omega$ , but we stipulate that  $\boldsymbol{\psi}_r(t) = \mathcal{O}(1)$ ,  $\omega \gg 1$ , for all  $r \in \mathbb{Z}_+$ . Knowing the structure of the forcing term, it seems reasonable to look for functions  $\boldsymbol{\psi}_r$  which are somehow related to modulated Fourier expansions. Before presenting the precise form of functions  $\boldsymbol{\psi}_r$  which occur in the DDE case, we need to

define the following sets,

$$\mathbb{M} = \{0\} \cup \{m \in \mathbb{Z} : \mathbf{a}_m \neq \mathbf{0} \text{ on } [0, T]\},$$

$$\mathbb{I}_r = \begin{cases} \{(0, m) : m \in \mathbb{M}\}, & r = 1, \\ \{(jm, m) : j \in \{0, 1, \dots, r-1\}, m \in \mathbb{M} \setminus \{0\}\} \cup \{(m, 0) : m \in \mathbb{M}\}, & r \geq 2. \end{cases}$$

The set  $\mathbb{M}$  consists of ‘active’ coefficients  $\mathbf{a}_m$ , while  $\mathbb{I}_r$  has no deep significance beyond making our notation simpler. The functions  $\psi_r$  for  $r \geq 1$  are of the form

$$\psi_r(t, \omega) = \sum_{(l, m) \in \mathbb{I}_r} \mathbf{b}_m^{r, l}(t) e^{i\omega(mt-l)}, \quad r \geq 1. \quad (2.4)$$

The major task ahead of us is to identify  $\mathbf{p}(t)$ ,  $t > 0$ , and  $\mathbf{b}_m^{r, l}$  for  $t \geq 0$ ,  $r \geq 1$ ,  $(l, m) \in \mathbb{I}_r$ .

### 2.3 Explicit form of the asymptotic expansion

In this subsection we are deriving explicit formulæ for the functions  $\mathbf{p}(t)$  and  $\mathbf{b}_m^{r, l}(t)$ ,  $r = 0, 1, \dots, \infty$ . For the convenience of reader and eventual application to the numerical solution of the DDE (1.1), it is convenient to obtain those coefficients in an algorithmic manner. The first few coefficients are in an explicit form

$$\begin{aligned} \mathbf{p}'(t) &= A\mathbf{p}(t) + B\mathbf{p}(t-1) + \mathbf{a}_0(t), \quad t \geq 0, \\ \mathbf{p}(t) &= \boldsymbol{\varphi}(t), \quad t \in [-1, 0); \end{aligned} \quad (2.5)$$

$$\begin{aligned} \mathbf{b}_m^{1, 0}(t) &= \frac{\mathbf{a}_m(t)}{im}, \quad m \neq 0, \\ \mathbf{b}_0^{1, 0'}(t) &= A\mathbf{b}_0^{1, 0}(t) + B\mathbf{b}_0^{1, 0}(t-1), \quad t \geq 0, \\ \mathbf{b}_0^{1, 0}(t) &\equiv \mathbf{0}, \quad t \in [-1, 0), \\ \mathbf{b}_0^{1, 0}(0) &= -\sum_{s \neq 0} \mathbf{b}_s^{1, 0}(0); \end{aligned} \quad (2.6)$$

$$\begin{aligned} \mathbf{b}_m^{2, 0}(t) &= \frac{1}{im} [A\mathbf{b}_m^{1, 0}(t) - \mathbf{b}_m^{1, 0'}(t)], \quad m \neq 0, \\ \mathbf{b}_m^{2, m}(t) &= \frac{1}{im} B\mathbf{b}_m^{1, 0}(t-1), \quad t > 0, \\ \mathbf{b}_0^{2, 0'}(t) &= A\mathbf{b}_0^{2, 0}(t) + B\mathbf{b}_0^{2, 0}(t-1), \quad t \geq 0, \\ \mathbf{b}_0^{2, 0}(t) &\equiv \mathbf{0}, \quad t \in [-1, 0), \\ \mathbf{b}_0^{2, 0}(0) &= -\sum_{s \neq 0} \mathbf{b}_s^{2, 0}(0); \\ \mathbf{b}_0^{2, m'}(t) &= A\mathbf{b}_0^{2, m}(t) + B\mathbf{b}_0^{2, m}(t-1), \quad t \geq 0, \quad m \neq 0, \\ \mathbf{b}_0^{2, m}(t) &\equiv \mathbf{0}, \quad t \in [-1, 0), \\ \mathbf{b}_0^{2, m}(0) &= -\mathbf{b}_m^{2, m}(0); \end{aligned}$$



$$\begin{aligned}
\mathbf{b}_m^{3,0}(t) &= \frac{1}{im} [A\mathbf{b}_m^{2,0}(t) - \mathbf{b}_m^{2,0'}(t)], \quad m \neq 0, \\
\mathbf{b}_m^{3,m}(t) &= \frac{1}{im} [A\mathbf{b}_m^{2,m}(t) + B\mathbf{b}_m^{2,0}(t-1) - \mathbf{b}_m^{2,m'}(t)], \quad m \neq 0, \\
\mathbf{b}_m^{3,2m}(t) &= \frac{1}{im} B\mathbf{b}_m^{2,m}(t-1), \quad m \neq 0
\end{aligned}$$

and so on. Note that  $\omega$  is completely absent from our formulæ! Thus, both the differential equations for  $\mathbf{p}$  and  $\mathbf{b}_0^{r,l}$  and the recursions for  $\mathbf{b}_m^{r,l}$ ,  $m \neq 0$ , are non-oscillatory.

The general expressions for the functions  $\mathbf{b}_m^{r,l}$  are

$$\begin{aligned}
\mathbf{b}_0^{r,0'}(t) &= A\mathbf{b}_0^{r,0}(t) + B\mathbf{b}_0^{r,0}(t-1), \quad t \geq 0, \\
\mathbf{b}_0^{r,0}(t) &\equiv 0, \quad t \in [-1, 0), \\
\mathbf{b}_0^{r,0}(0) &= -\sum_{s \neq 0} \mathbf{b}_s^{r,0}(0);
\end{aligned} \tag{2.7}$$

$$\begin{aligned}
\mathbf{b}_0^{r,m'}(t) &= A\mathbf{b}_0^{r,m}(t) + B\mathbf{b}_0^{r,m}(t-1), \quad t \geq 0, \quad m \neq 0, \\
\mathbf{b}_0^{r,m}(t) &\equiv 0, \quad t \in [-1, 0), \\
\mathbf{b}_0^{r,m}(0) &= -\sum_{j=1}^{r-1} \mathbf{b}_m^{r,jm}(0),
\end{aligned} \tag{2.8}$$

$$\mathbf{b}_m^{r,0}(t) = \frac{1}{im} [A\mathbf{b}_m^{r-1,0}(t) - \mathbf{b}_m^{r-1,0'}(t)], \quad m \neq 0; \tag{2.9}$$

$$\begin{aligned}
\mathbf{b}_m^{r,jm}(t) &= \frac{1}{im} [A\mathbf{b}_m^{r-1,jm}(t) + B\mathbf{b}_m^{r-1,(j-1)m}(t-1) - \mathbf{b}_m^{r-1,jm'}(t)], \\
m \neq 0, \quad j &= 1, 2, \dots, r-2,
\end{aligned} \tag{2.10}$$

$$\mathbf{b}_m^{r,(r-1)m}(t) = \frac{1}{im} B\mathbf{b}_m^{r-1,(r-2)m}(t-1), \quad m \neq 0 \tag{2.11}$$

for all  $r \geq 1$ , except for  $r = 1, l = 0, m \neq 0$ , which has been already given by (2.6).

The beauty and power of expressions (2.5–11) lies in their simplicity. Note that a single complicated, highly oscillatory delayed differential equation is replaced with recursive equations or delay differential equations which, being non-oscillatory, can be easily solved numerically with standard methods. Of course, practical application of (2.3) to numerical computation requires the truncation of the infinite sum, but this can be done in a transparent manner and, as we see in Section 3, restricting  $r$  to a very small range already yields an excellent approximation – one whose excellence *improves* once  $\omega$  becomes larger.

We now proceed to derive (2.5–11) in a systematic manner. For simplicity of notation we henceforth omit the dependence on  $t$  of the functions in question and adopt the convention that placing a tilde on the top of a function means that it is evaluated at point  $t-1$ . Hence,  $\mathbf{p}$  should be understood as  $\mathbf{p}(t)$ , while  $\tilde{\mathbf{p}}$  stands for  $\mathbf{p}(t-1)$ .

Applying *ansatz* (2.2) to the equation (1.1) we obtain

$$\begin{aligned}
& \mathbf{p}' + \sum_{(l,m) \in \mathbb{I}_1} i m \mathbf{b}_m^{1,l} e^{i\omega(nt-l)} \\
& + \sum_{r=1}^{\infty} \frac{1}{\omega^r} \left[ \sum_{(l,m) \in \mathbb{I}_r} \mathbf{b}_m^{r,l'} e^{i\omega(mt-l)} + \sum_{(l,m) \in \mathbb{I}_{r+1}} i m \mathbf{b}_m^{r+1,l} e^{i\omega(mt-l)} \right] \\
& = A \left[ \mathbf{p} + \sum_{r=1}^{\infty} \frac{1}{\omega^r} \sum_{(l,m) \in \mathbb{I}_r} \mathbf{b}_m^{r,l} e^{i\omega(mt-l)} \right] + B \left[ \tilde{\mathbf{p}} + \sum_{r=1}^{\infty} \frac{1}{\omega^r} \sum_{(l,m) \in \mathbb{I}_r} \tilde{\mathbf{b}}_m^{r,l} e^{i\omega(mt-l-m)} \right] \\
& + \sum_{m \in \mathbb{M}} \mathbf{a}_m e^{i\omega mt}.
\end{aligned} \tag{2.12}$$

We identify above two different kinds of scales: *magnitude*, expressed in power of  $\omega$ , and *frequency*, namely terms of the form  $e^{i\omega mt}$  for distinct  $m$ . The first stage is to separate magnitudes and, next, separate frequencies. We let

$$\tilde{\mathbb{I}}_r = \{(l, m) \in \mathbb{I}_r : m \neq 0\} \subset \mathbb{I}_r, \quad r \in \mathbb{N}.$$

### 2.3.1 The zeroth term

We commence by collecting the  $\mathcal{O}(1)$  (in  $\omega$ ) terms in (2.12). The outcome is

$$\mathbf{p}' + \sum_{(l,m) \in \tilde{\mathbb{I}}_1} i m \mathbf{b}_m^{1,l} e^{i\omega(mt-l)} = A \mathbf{p}(t) + B \mathbf{p}(t-1) + \mathbf{a}_0(t) + \sum_{m \in \mathbb{M} \setminus \{0\}} \mathbf{a}_m e^{i\omega mt}.$$

Next we separate frequencies.  $m = 0$  yields (2.5), while  $m \in \tilde{I}_1$  results in (2.6).

### 2.3.2 The $r = 1$ term

Now we pull out of (2.12) the coefficients of magnitude  $\mathcal{O}(\omega^{-1})$ . The outcome is

$$\begin{aligned}
& \sum_{(l,m) \in \mathbb{I}_1} \mathbf{b}_m^{1,l'} e^{i\omega(mt-l)} + \sum_{(l,m) \in \mathbb{I}_2} i m \mathbf{b}_m^{2,l} e^{i\omega(mt-l)} \\
& = A \sum_{(l,m) \in \mathbb{I}_1} \mathbf{b}_m^{1,l} e^{i\omega(mt-l)} + B \sum_{(l,m) \in \mathbb{I}_1} \tilde{\mathbf{b}}_m^{1,l} e^{i\omega(mt-l-m)}.
\end{aligned}$$

Since  $\mathbb{I}_1 = \{(0, m); m \in \mathbb{M}\}$  and  $\mathbb{I}_2 = \{(0, m), (m, m), (m, 0); m \in \mathbb{M}\}$ , this is equivalent to

$$\begin{aligned}
& \sum_{(0,m) \in \tilde{\mathbb{I}}_1} \mathbf{b}_m^{1,0'} e^{i\omega mt} + \sum_{(0,0) \in \mathbb{I}_1} \mathbf{b}_0^{1,0'} + \sum_{(m,m) \in \mathbb{I}_2 \setminus \mathbb{I}_1} i m \mathbf{b}_m^{2,m} e^{i\omega m(t-1)} + \sum_{(0,m) \in \tilde{\mathbb{I}}_1} i m \mathbf{b}_m^{2,0} e^{i\omega mt} \\
& = A \sum_{(0,m) \in \tilde{\mathbb{I}}_1} \mathbf{b}_m^{1,0} e^{i\omega mt} + A \sum_{(0,0) \in \mathbb{I}_1} \mathbf{b}_0^{1,0} + B \sum_{(0,m) \in \tilde{\mathbb{I}}_1} \tilde{\mathbf{b}}_m^{1,0} e^{i\omega m(t-1)} + B \sum_{(0,0) \in \mathbb{I}_1} \tilde{\mathbf{b}}_0^{1,0}.
\end{aligned}$$

Bearing in mind the definitions of  $\mathbb{I}_1$ ,  $\mathbb{I}_2$  and  $\tilde{\mathbb{I}}_1$ , we thus have

$$\begin{aligned} \mathbf{b}_0^{1,0'} &= A\mathbf{b}_0^{1,0} + B\tilde{\mathbf{b}}_0^{1,0}, \\ \mathbf{b}_m^{2,0} &= \frac{1}{im}[A\mathbf{b}_m^{1,0} - \mathbf{b}_m^{1,0'}], \quad m \neq 0, \\ \mathbf{b}_m^{2,m} &= \frac{1}{im}B\tilde{\mathbf{b}}_m^{1,0}, \quad m \neq 0, \end{aligned}$$

consistently with (2.7), (2.9) and (2.11), respectively. Finally, the initial conditions for  $\mathbf{b}_0^{1,0}$  follow from the condition

$$\psi_r(t, \omega) \equiv 0, \quad t \in [-1, 0], \quad r \geq 1, \quad (2.13)$$

which is implied by  $\mathbf{p}(t) = \boldsymbol{\varphi}(t)$ ,  $t \in [-1, 0]$ , and  $\psi_r = \mathcal{O}(1)$ ,  $\omega \gg 1$ .

### 2.3.3 The $r = 2$ term

We note the pattern: for any  $r$  we obtain a DDE for  $\mathbf{b}_0^{r,l}$  and recurrence relations for  $\mathbf{b}_m^{r+1,l}$ ,  $m \neq 0$ . This is also the case for  $r = 2$ . Collecting  $\mathcal{O}(\omega^{-2})$  terms, we thus have

$$\begin{aligned} & \sum_{(0,m) \in \tilde{\mathbb{I}}_2} \mathbf{b}_m^{2,0'} e^{i\omega m t} + \sum_{(m,m) \in \tilde{\mathbb{I}}_2} \mathbf{b}_m^{2,m'} e^{i\omega m(t-1)} + \sum_{(l,0) \in \mathbb{I}_2 \setminus \tilde{\mathbb{I}}_2} \mathbf{b}_0^{2,l'} e^{-i\omega l} + \mathbf{b}_0^{2,0'} \\ & + \sum_{(0,m) \in \tilde{\mathbb{I}}_2} im \mathbf{b}_m^{3,0} e^{im\omega t} + \sum_{(m,m) \in \tilde{\mathbb{I}}_2} im \mathbf{b}_m^{3,m} e^{i\omega m(t-1)} + \sum_{(2m,m) \in \tilde{\mathbb{I}}_3} im \mathbf{b}_m^{3,2m} e^{i\omega m(t-2)} \\ & = A \sum_{(0,m) \in \tilde{\mathbb{I}}_2} \mathbf{b}_m^{2,0} e^{i\omega m t} + A \sum_{(l,0) \in \mathbb{I}_2} \mathbf{b}_0^{2,l} e^{-i\omega l} + A \sum_{(m,m) \in \mathbb{I}_2} \mathbf{b}_m^{2,m} e^{i\omega m(t-1)} + A\mathbf{b}_0^{2,0} \\ & + B \sum_{(0,m) \in \tilde{\mathbb{I}}_2} \tilde{\mathbf{b}}_m^{2,0} e^{i\omega m(t-1)} + B \sum_{(l,0) \in \mathbb{I}_2} \tilde{\mathbf{b}}_0^{2,l} e^{-i\omega l} + B \sum_{(m,m) \in \mathbb{I}_2} \tilde{\mathbf{b}}_m^{2,m} e^{i\omega m(t-2)} + B\tilde{\mathbf{b}}_0^{2,0}, \end{aligned}$$

where  $\mathbb{I}_3 = \{(0, m), (m, m), (2m, m), (m, 0) : m \in \mathbb{M}\}$ .

Separating frequencies, we have the following:

$$\begin{aligned} e^{-i\omega m} : \quad & \mathbf{b}_0^{2,m'} = A\mathbf{b}_0^{2,m} + B\tilde{\mathbf{b}}_0^{2,m}, \quad m \in \mathbb{Z}, \\ e^{im\omega t} : \quad & \mathbf{b}_m^{3,0} = \frac{1}{im}(A\mathbf{b}_m^{2,0} - \mathbf{b}_m^{2,0'}), \quad m \neq 0, \\ e^{i\omega m(t-1)} : \quad & \mathbf{b}_m^{3,m} = \frac{1}{im}(A\mathbf{b}_m^{2,m} + B\tilde{\mathbf{b}}_m^{2,m} - \mathbf{b}_m^{2,m'}), \quad m \neq 0, \\ e^{i\omega m(t-2)} : \quad & \mathbf{b}_m^{3,2m} = \frac{1}{im}B\tilde{\mathbf{b}}_m^{2,m}, \quad m \neq 0. \end{aligned}$$

The initial conditions for the DDEs follow from (2.13) and all is consistent with (2.7–11).

### 2.3.4 The $r$ -th term

We have already done the heavy lifting: the general case follows identically to  $r = 2$ . Thus,

$$\mathbb{I}_{r-1} = \{(0, m), (m, m), \dots, ((r-2)m, m), (m, 0) : m \in \mathbb{M}\}$$

and

$$\begin{aligned}
& \sum_{j=0}^{r-1} \sum_{m \neq 0} \mathbf{b}_m^{r,jm'} e^{i\omega m(t-j)} + \sum_{m=-\infty}^{\infty} \mathbf{b}_0^{r,m'} e^{-i\omega m} + \sum_{j=0}^r \sum_{m \neq 0} i m \mathbf{b}_m^{r+1,jm} e^{im\omega(t-j)} \\
&= A \sum_{j=0}^{r-1} \sum_{m=-\infty}^{\infty} \mathbf{b}_m^{r,jm} e^{i\omega m(t-j)} + A \sum_{m=-\infty}^{\infty} \mathbf{b}_0^{r,m} e^{-i\omega m} \\
&+ B \sum_{j=1}^r \sum_{m=-\infty}^{\infty} \tilde{\mathbf{b}}_m^{r,(j-1)m} e^{im\omega(t-j)} + B \sum_{m=-\infty}^{\infty} \tilde{\mathbf{b}}_0^{r,m} e^{-i\omega m}.
\end{aligned}$$

Again we separate the frequencies and the outcome is

$$\begin{aligned}
e^{-i\omega m} : \quad & \mathbf{b}_0^{r,m'} = A \mathbf{b}_0^{r,m} + B \tilde{\mathbf{b}}_0^{r,m}, \quad m \in \mathbb{Z}, \\
e^{i\omega m t} : \quad & \mathbf{b}_m^{r+1,0} = \frac{1}{im} (A \mathbf{b}_m^{r,0} - \mathbf{b}_m^{r,0'}), \quad m \neq 0, \\
e^{i\omega m(t-j)} : \quad & \mathbf{b}_m^{r+1,jm} = \frac{1}{im} (A \mathbf{b}_m^{r,jm} + B \tilde{\mathbf{b}}_m^{r,(j-1)m} - \mathbf{b}_m^{r,jm'}), \quad j = 1, \dots, r-1, \quad m \neq 0, \\
e^{i\omega m(t-r)} : \quad & \mathbf{b}_m^{r+1,rm} = \frac{1}{im} B \tilde{\mathbf{b}}_m^{r,(r-1)m}, \quad m \neq 0.
\end{aligned}$$

This, together with initial conditions derived from (2.13), is precisely (2.7–11) with appropriately shifted index  $r$ , confirming the validity of the DDEs and recurrence relations which, in their totality, result in the asymptotic expansion (2.3–4).

## 2.4 An asymptotic-numerical method

The numerical implementation of the asymptotic expansion (2.3–4) requires three different truncations. Firstly, we need to replace the right-hand side of (2.3) by a finite sum,

$$\mathbf{y}(t) \approx \mathbf{p}(t) + \sum_{r=1}^p \frac{1}{\omega^r} \psi_r(t, \omega). \quad (2.14)$$

Note that fairly small values of  $p \geq 1$  are perfectly adequate: in Section 1 we have used  $p = 1$  even with fairly small  $\omega$ , yet the results were very good indeed. Secondly, we need to restrict the set  $\mathbb{M}$ , hence also  $\mathbb{I}_r$ ,  $r = 1, \dots, p$  to

$$\mathbb{M}_s = \{m \in \mathbb{M} : |m| \leq s\}$$

for suitably large  $s \geq 1$ . Note that many sets  $\mathbb{M}$  in applications are already finite and there is no need to truncate them. Finally, we need to solve (2.5) and (2.7–8) numerically: given that these are non-oscillatory linear DDEs, this can be done with great ease using existing methods and software.

Note that, at least in principle, we can use just one expansion (2.14) in the entire interval of interest  $[0, T]$ . This is not a good idea: (2.3) is an asymptotic expansion, hence we cannot be assured of convergence in exceedingly long intervals. Although precise analysis, even in an ODE case, is not yet available, computational experience indicates that a good policy is to cover  $[0, T]$  with a fairly small number of large time steps. In each time step we re-compute the functions  $\mathbf{p}$  and  $\mathbf{b}_m^{r,l}$  in the requisite range – of course, we no longer start at the origin, but this represents no problem whatsoever.

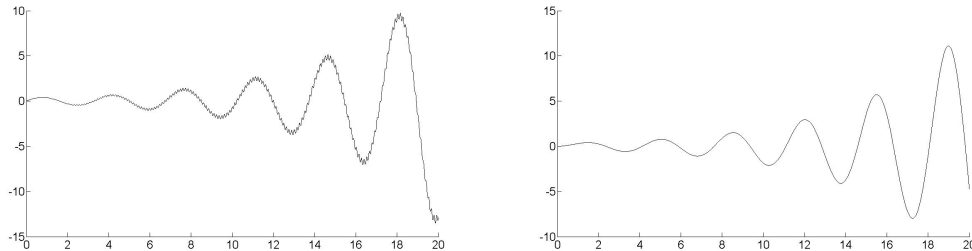


Figure 3.1: The real and imaginary parts of the solution of (3.1) for  $\omega = 50$ .

### 3 Few examples

It is a sound policy to try any new computational tool on a number of examples: although general theory assures us of the efficacy of our approach, numerical experimentation might well highlight potential problems. Moreover, in the case of DDEs (1.1), there is very little experience which sort of solution to expect, hence the merit in using the approach of Section 2 as an exploratory tool.

All computations in this section have been performed using (2.14) with  $p = 6$ . The DDEs, required to derive expansion terms in (2.14), have been computed with `dde23` using very small bound on absolute error. Given that these DDEs are all non-oscillatory, this has resulted in very small – practically, negligible – global error and the computation itself is extraordinarily rapid.

We commence from the scalar equation

$$\begin{aligned} y'(t) &= iy(t) - y(t-1) + t \sin \omega t, & 0 < t \leq 20, \\ y(t) &= e^{it}, & -1 \leq t \leq 0. \end{aligned} \quad (3.1)$$

The forcing term can be easily represented as a modulated Fourier series,  $a_{-1}(t) = \frac{1}{2}it$ ,  $a_1(t) = -\frac{1}{2}it$ ,  $a_m \equiv 0$  for  $|m| \neq 1$ . Note that the amplitude of the forcing term grows linearly and we expect to see this expressed in the exact solution.

We commence from a fairly modest oscillation,  $\omega = 50$ . The real and imaginary parts of the solution are displayed in Fig. 3.1. It is evident that the amplitude lives within a linearly-increasing envelope, in line with the linear increase in the amplitude of the forcing term. Moreover, it can be easily seen that the solution consists of a smooth component overlaid by small-amplitude rapid oscillations: all this is in line with the theory of the last section. (The oscillations are easily visible only in the real part, but this is purely a matter of plotting resolution: read on.)

Next we increase  $\omega$  in (3.1) two hundred-fold, to  $\omega = 10000$ . We are now within a regime that is bound to defeat standard numerical methods: bearing in mind the discussion in Section 1, a reasonable choice of step-size  $h > 0$  in a classical numerical method must satisfy  $h\omega \ll 1$ . Indeed, wishing to obtain an error less than a user-supplied tolerance `TOL`, a good rule of a thumb is to choose  $h = \rho \cdot \text{TOL}^{1/p} \omega^{-1}$ , where  $p$  is the (classical) order of the classical method and  $\rho \in (0, 1)$ . In the case of the Euler method of Section 1, `TOL` =  $10^{-6}$  means  $h < 10^{-10}$ . This leads to prohibitive

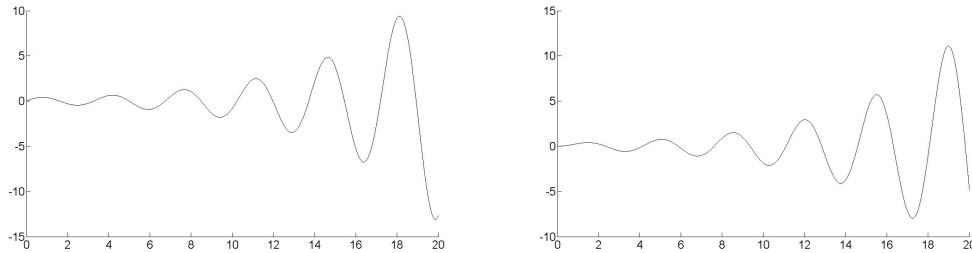


Figure 3.2: The real and imaginary parts of the solution of (3.1) for  $\omega = 10^4$ .

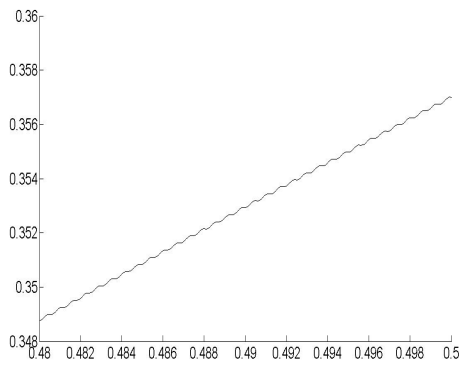


Figure 3.3: The real part of the solution of (3.1) for  $\omega = 10^4$  in a very small sub-interval: note that the oscillations are now visible.

cost. Worse, given the sheer number of floating-point operations, such a small step-size results in very significant round-off error, which is bound to render any estimate of global error fairly meaningless.

Unlike classical methods, the asymptotic-numerical solver (2.14) remains robust – actually, improves – for large  $\omega$ , while the run-time (for fixed  $p$ ) is independent of  $\omega$ . Real and imaginary parts of the solution are displayed in Fig. 3.2.

Comparing Figs 3.1 and 3.2, we note that the solution is almost identical, the only difference being that the small-amplitude oscillations in Fig. 3.1 seem to have disappeared altogether in Fig. 3.2. This, of course, is an illusion: the oscillations have not gone away, their amplitude just became *very* small indeed, roughly  $\approx 10^{-4}t$ . Thus, they are simply too small to be seen in Fig. 3.2. However, once we focus on a much smaller time interval, the oscillations are visible with the naked eye. Thus, in Fig. 3.3 we have displayed the solution of (3.1) with  $\omega = 10^4$  in a very small time interval. Because the function  $p(t)$  varies there very moderately, small-amplitude oscillations overlaying it can be easily seen. Of course, the fact that we cannot see the oscillations does not mean that somehow they are ‘invisible’ to a classical numerical method.

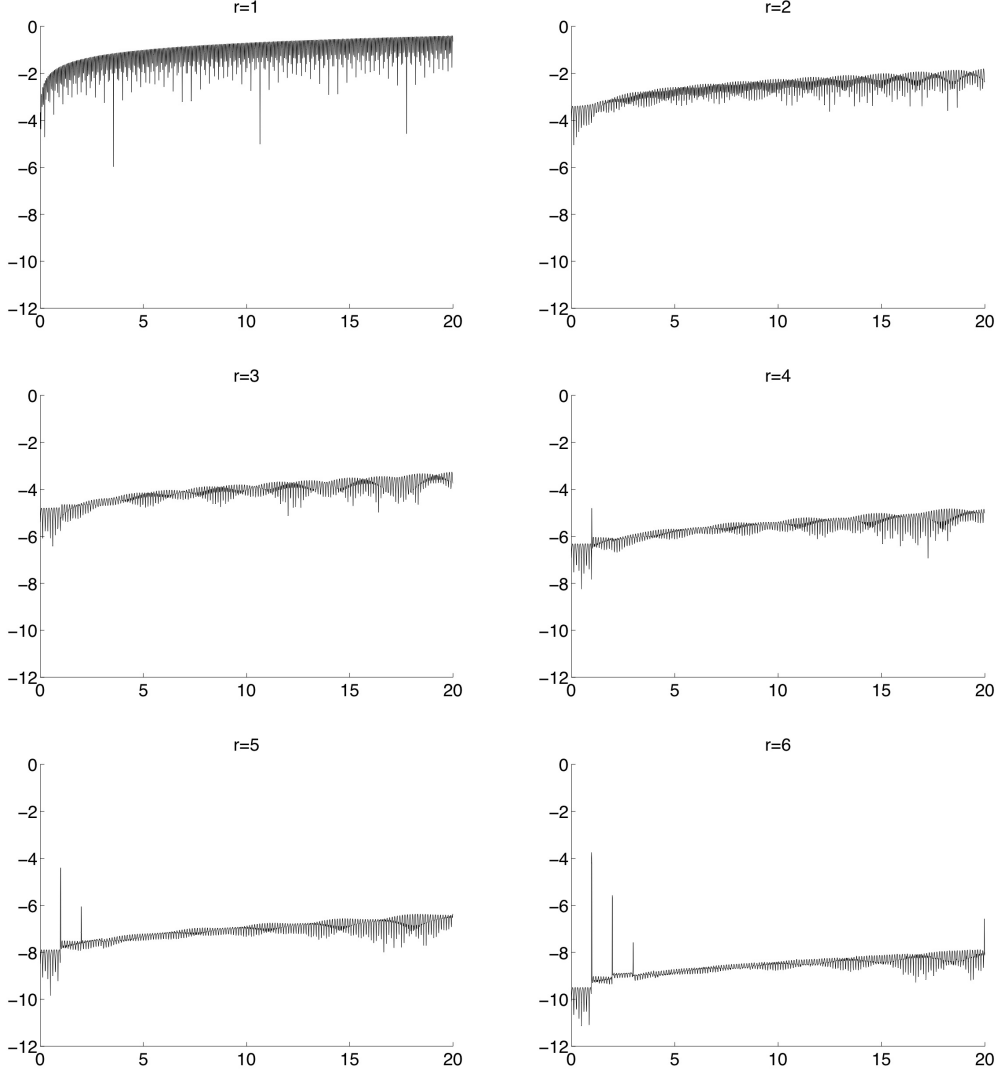


Figure 3.4: The size  $\log_{10} |\psi_r(t, \omega)|$  of the consecutive ‘layers’ in (2.14) for equation (3.1) with  $\omega = 10^4$ .

In Fig. 3.4 we have displayed the size of the ‘layers’ in formula (2.14), i.e. plotted  $\log_{10} |\psi_r(t, \omega)|$  for equation (3.1),  $\omega = 10^4$  and  $r = 1, \dots, 6$ . To illustrate the rate of decay in the amplitude for increasing  $r$ , we have plotted all graphs with the same vertical axis. The oscillation is evident – as is evident that the amplitude decreases with  $r$ , in line with the reasoning underlying our methodology. We also observe that for large  $rs$  there are unwelcome jumps in amplitude at integer points and that the

size these jumps decays rapidly as the time increases. Although no comprehensive explanation of this behaviour is available, it makes sense that it is connected to the regularity of the solutions of DDEs: it is well known that that  $k$ th derivative of  $\mathbf{y}$  in (1.1) may be discontinuous at  $t = k$ ,  $k \in \mathbb{Z}_+$ . The likely culprit is not the formula (2.14) *per se* but a deterioration in the accuracy of the numerical method used to solve the non-oscillatory systems (2.5), (2.7) and (2.8) at integer points.

Our last example is the highly oscillatory DDE system (1.1), where

$$\begin{aligned} A &= \begin{bmatrix} -2 & 1 & 0 \\ 1 & -2 & 1 \\ 0 & 1 & -2 \end{bmatrix}, \quad B = \begin{bmatrix} 0 & 1 & 0 \\ -1 & 0 & 0 \\ 0 & 0 & -1 \end{bmatrix}, \\ \mathbf{a}_{-2} &= \begin{bmatrix} 0 \\ 0 \\ -2 \end{bmatrix}, \quad \mathbf{a}_0 = \begin{bmatrix} 0 \\ -1 \\ 1 \end{bmatrix}, \quad \mathbf{a}_1 = \begin{bmatrix} \frac{1}{2} \\ 0 \\ 0 \end{bmatrix}, \quad \mathbf{a}_2 = \begin{bmatrix} 0 \\ \cos t \\ 0 \end{bmatrix}, \quad \mathbf{a}_3 = \begin{bmatrix} 0 \\ 0 \\ \frac{1}{2} \end{bmatrix}, \end{aligned} \quad (3.2)$$

otherwise  $\mathbf{a}_m = \mathbf{0}$ , with zero initial condition in  $(-1, 0]$ .

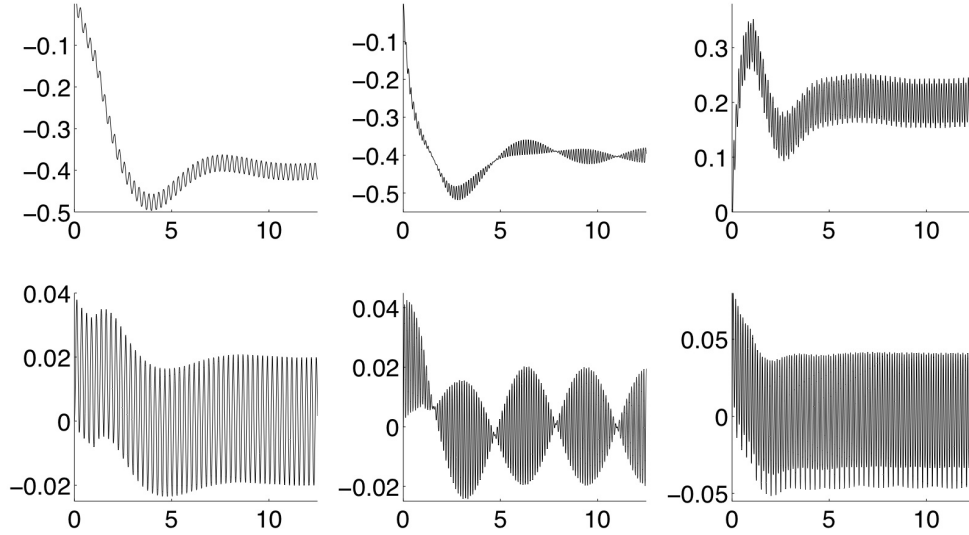


Figure 3.5: Real (top row) and imaginary parts of the three components of the solution of the system (3.2) with  $\omega = 25$ , using  $p = 6$ .

Figs 3.5–7 exhibit the solution of the highly oscillatory DDE system (3.2) for three different values of  $\omega$ . In each case we have used  $p = 6$ , solving non-oscillatory equations with `dde23` to very high accuracy. The oscillation in Fig. 3.5 is fairly mild and, as we should already come to expect, it is of a fairly large amplitude. The amplitude is roughly halved in Fig. 3.6, once the frequency  $\omega$  is doubled (this behaviour is much



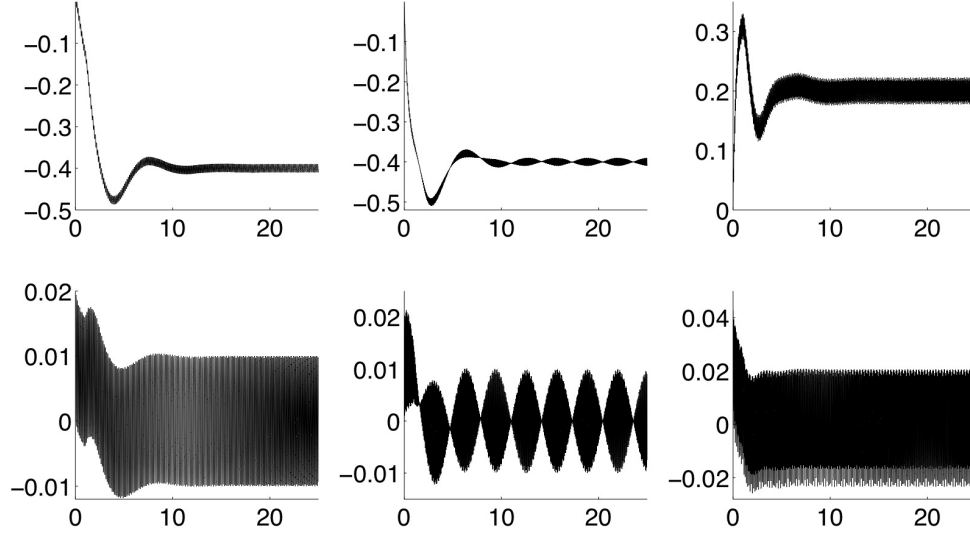


Figure 3.6: Real (top row) and imaginary parts of the three components of the solution of the system (3.2) with  $\omega = 50$ , using  $p = 6$ .

more visible for the imaginary part, in the bottom row, which oscillates about the zero solution). It is halved again in Fig. 3.7, consistently with our theory.

## 4 Conclusions

This paper represents a preliminary exploration of the very rich and unexplored area of delay-differential equations with highly oscillatory forcing. We have demonstrated that the solution of the linear system  $\mathbf{y}'(t) = A\mathbf{y}(t) + B\mathbf{y}(t-1) + \sum_{m=-\infty}^{\infty} \mathbf{a}_m(t)e^{im\omega t}$  can be expanded into asymptotic series in inverse powers of the frequency  $\omega$  and that this expansion can be used as a cornerstone of a very effective numerical method.

The next stage in the exploration of DDEs with highly oscillatory forcing terms ventures into the realm of nonlinear equations of the form

$$\mathbf{y}'(t) = \mathbf{f}(t, \mathbf{y}(t), \mathbf{y}(t-1)) + \sum_{m=-\infty}^{\infty} \mathbf{a}_m(t)e^{im\omega t}.$$

We expect to explore this issue in a future paper. Another outstanding challenge is to incorporate our theory, whether for linear or nonlinear DDEs, into practical applications in computational electronic engineering.

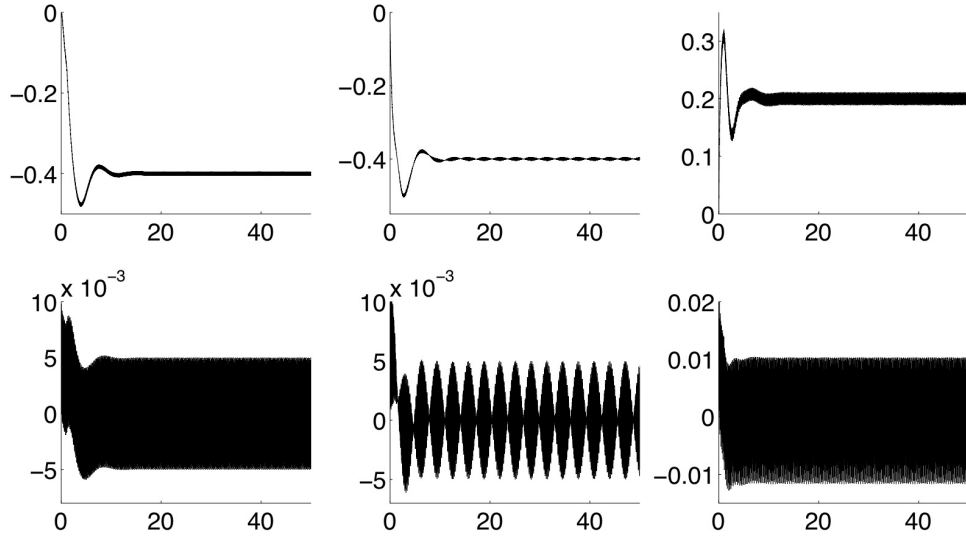


Figure 3.7: Real (top row) and imaginary parts of the three components of the solution of the system (3.2) with  $\omega = 100$ , using  $p = 6$ .

## References

- Bellen, A. & Zennaro, M. (2003), *Numerical Methods for Delay Differential Equations*, Oxford University Press, Oxford, UK.
- Calvo, M. P. & Sanz-Serna, J. M. (2010), ‘Heterogeneous multiscale methods for mechanical systems with vibrations’, *SIAM J. Sci. Comput.* **32**, 2029–2046.
- Chartier, P., Murua, A. & Sanz-Serna, J. M. (2010), ‘Higher-order averaging, formal series and numerical integration I: B-series’, *Found. Comp. Maths* **10**, 695–727.
- Chembo, Y. K., Larger, L. & Colet, P. (2008), ‘Nonlinear dynamics and spectral stability of optoelectronic microwave oscillators’, *IEEE J. Quantum Electronics* **44**, 858–866.
- Cohen, D., Hairer, E. & Lubich, C. (2005), ‘Modulated Fourier expansions of highly oscillatory differential equations’, *Found. Comp. Maths* **3**, 327–450.
- Condon, M., Deaño, A. & Iserles, A. (2010a), ‘On second order differential equations with highly oscillatory forcing terms’, *Proc. Royal Soc. A* **466**, 1809–1828.
- Condon, M., Deaño, A. & Iserles, A. (2010b), ‘On systems of differential equations with extrinsic oscillation’, *Discr. and Cont. Dynamical Sys.* **28**, 1345–1367.

- Engquist, B., Fokas, A., Hairer, E. & Iserles, A., eds (2009), *Highly Oscillatory Problems*, Cambridge University Press, Cambridge, UK.
- Kyrychko, Y. N. & Hogan, S. J. (2010), ‘On the use of delay equations in engineering applications’, *J. Vibration & Control* **16**, 943–960.
- Udaltsov, V. S., Goedgebuer, J. P., Larger, L., Cuenot, J. B., Levy, P. & Rhodes, W. T. (2003), ‘Cracking chaos-based encryption systems ruled by nonlinear time delay differential equations’, *Physics Lett. A* **308**, 54–60.
- van Wiggeren, G. D. & Roy, R. (1998), ‘Communication with chaotic lasers’, *Science* **279**, 1198–1200.
- Wirkus, S. & Rand, R. (2002), ‘The dynamics of two coupled van der pol oscillators with delay coupling’, *Nonlinear Dynamics* **30**, 205–221.